Synthesis and structural investigations of *N*-alkylated β-peptidosulfonamide–peptide hybrids of the amyloidogenic amylin(20–29) sequence: implications of supramolecular folding for the design of peptide-based bionanomaterials

Ronald C. Elgersma,[a] Tania Meijneke,[a] Remco de Jong,[a] Arwin J. Brouwer,[a] George Posthuma,[b] Dirk T. S. Rijkers[a] and Rob M. J. Liskamp*[a]

Received 15th May 2006, Accepted 27th July 2006
First published as an Advance Article on the web 21st August 2006
DOI: 10.1039/b606875h

The incorporation of a single β-aminoethane sulfonyl amide moiety in a highly amyloidogenic peptide sequence resulted in a complete loss of amyloid fibril formation. Instead, supramolecular folding morphologies were observed. Subsequent chemoselective *N*-alkylation of the sulfonamide resulted in amphiphilic peptide-based hydrogelators. It was found that variation of merely the alkyl chain induced a dramatic variation in aggregation motifs such as helical ribbons and tapes, ribbons progressing to closed tubes, twisted lamellar sheets and entangled/branched fibers.

Introduction

The incorporation of peptide backbone amide bond isosteres has a tremendous influence on the folding behavior and biochemical/biophysical properties of the native peptide sequence. Well known examples of such amide bond isosteres are, among others: esters (resulting in depsipeptides),[1] peptoids (*N*-alkyl glycines),[2] peptido-ureas,[3] peptoid ureas,[4] alkene dipeptide isosteres,[5] β-peptidosulfonamides[6] and peptoid sulfonamides.[7] Recently, we have shown that replacement of one or more backbone amide bonds by ester- or peptoid moieties, respectively, within amyloidogenic peptide sequences abrogated their amyloid fibril-forming properties.[8]

Since the seminal publications of β-peptides by Seebach[9] and Gellman,[10] this concept has found many applications in the design of peptide sequences with novel folding characteristics (foldamers),[11] antimicrobial properties and biological activities as receptor (ant)agonists and enzyme inhibitors.[12] Rather unexpectedly, extension of the backbone within an α-amino acid residue by a single methylene moiety (thus leading to β-amino acids) results in a hydrogen bonding network which stabilizes the secondary structures of relatively short β-peptides (Fig. 1).[10] An attractive feature of β-peptidosulfonamides compared to β-peptides is the identical number of atoms in each backbone residue (Fig. 1). This allows unequivocal conclusions regarding the influence of the sulfonamide moiety in β-peptidosulfonamides oligomers[13] and hybrids of β-peptidosulfonamide–β-peptides and β-peptidosulfonamide–α-peptides, respectively. In this context we have shown earlier that the incorporation of a single β-peptidosulfonamide moiety in a hexameric- or nonameric β-peptide completely attenuates the helical structure of these β-peptides,[14] thus the β-peptidosulfonamide moiety acts as a helix breaker entity.

This helix breaker property of the β-peptidosulfonamide moiety triggered us to study the incorporation of β-peptidosulfonamides into peptide sequences with a high tendency to form (anti)parallel β-sheets. Incorporation of a single β-aminoethane sulfonyl amide moiety in an all α-amino acid peptide sequence introduces an extra methylene group, thus inducing an out of register hydrogen bonding network compared to an antiparallel β-sheet. Moreover, the sulfonamide *O*-atoms are poor hydrogen bond acceptors but the increased acidity of the sulfonamide N*H* makes it a better hydrogen bond donor compared to a peptide amide moiety.[15] This dichotomy of hydrogen bond acceptor/donor properties can be used for the design of soluble β-sheet mimics.

[a]*Department of Medicinal Chemistry and Chemical Biology, Utrecht Institute for Pharmaceutical Sciences, Utrecht University, PO Box 80082, 3508 TB, Utrecht, The Netherlands. E-mail: R.M.J.Liskamp@pharm.uu.nl; Fax: +31 (0)30 2536655; Tel: +31 (0)30 2537396*
[b]*Department of Cell Biology, Center for Electron Microscopy, University Medical Center, 3508 GA, Utrecht, The Netherlands*

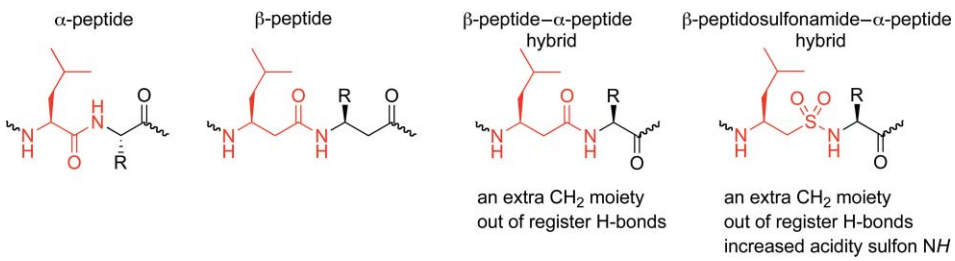

Fig. 1 Structures of an α-peptide, β-peptide, β-peptide–α-peptide hybrid and β-peptidosulfonamide–α-peptide hybrid.

Recently, we have found that modification of the peptide backbone of the highly amyloidogenic peptide amylin(20–29) does not form amyloid fibrils.[8] However, due to the increased hydrophobicity of these newly designed amylin(20–29) peptides, they self-assemble into large helical ribbons and peptide nanotubes.[8b] These amyloid-based peptides can be used as novel hydrogelators in the design of bionanomaterials.[16] In recent reviews[17] some general properties of molecules, which are thought to act as hydrogelators, have been defined. To gel a solvent (and in particular, water) an amphiphilic molecule with a hydrophobic functionality to promote aggregation and hydrophilic or charged groups to provide solubility is required.[17a] As stated above, in β-peptidosulfonamide–α-peptide hybrids, the increased acidity of the sulfonamide N*H* is particularly useful for the chemoselective and regiospecific alkylation of the peptide backbone.[18] This alkylation will result in two novel properties of these β-peptidosulfonamide–α-peptide molecular constructs. First, removal of a hydrogen bond donor to disrupt amyloid formation and second, introduction of an alkyl chain to tune hydrophobicity and thus to optimize their hydrogelation properties for material design based on self-assembly.

Here, we describe that the incorporation of a single β-aminoethane sulfonyl amide moiety in the amylin(20–29) peptide sequence resulted in a complete loss of amyloid fibril formation, instead the formation of hydrogels and supramolecular folding morphologies was observed. Subsequent *N*-alkylation of the sulfonamide resulted in a variety of aggregation motifs such as helical ribbons and tapes, ribbons progressing to closed tubes, twisted lamellar sheets and entangled/branched fibers. These desired properties will be used to design self-assembled bionanomaterials of amyloid-derived peptides.[16]

Results

Synthesis

The assembly of the amylin(20–29) peptides **1**–**4** and the on-resin Mitsunobu alkylations are shown in Scheme 1. The resin-bound protected dipeptide H–Ser(*t*-Bu)–Ser(*t*-Bu) was treated with the *N*-β-Fmoc-protected β-aminoethane sulfonyl chloride derivative of leucine[19] in the presence of *N*-methylmorpholine in dichloromethane. These reaction conditions have been recently described by us for the synthesis of oligo-β-peptidosulfonamides.[13,14] Then, the synthesis proceeded following the Fmoc/*t*-Bu solid phase peptide synthesis protocols.[20] The final amino acid was introduced as an *N*-α-Boc protected derivative (Boc–Ser(*t*-Bu)–OH), since the basic conditions during the Mitsunobu alkylations (*vide infra*) were not completely orthogonal with an Fmoc group, moreover, the final peptides should have a free α-amino functionality.

The increased acidity of the sulfonyl amide N*H* was used for a regioselective alkylation of the peptide backbone.[18] Electrophiles, *e.g.* allylic- or benzylic bromides, were used in the presence of several bases (DBU, DABCO, K_2CO_3 and TEA), however, HPLC- and mass analyses of the resulting peptides were not satisfactory with respect to purity and identity. Therefore, these alkylations were carried out by the Mitsunobu reaction,[21] thereby broadening the scope of the possible alkyl chains, since a diverse set of alcohols can be used. It turned out that the alkylation proceeded smoothly and a large variety of alcohols could be used (Fig. 2).

After treatment with TFA, to remove all protecting groups and to detach the peptide from the resin, the *N*-alkylated β-peptidosulfonamide–peptide hybrids **4a**–**l** were obtained in good

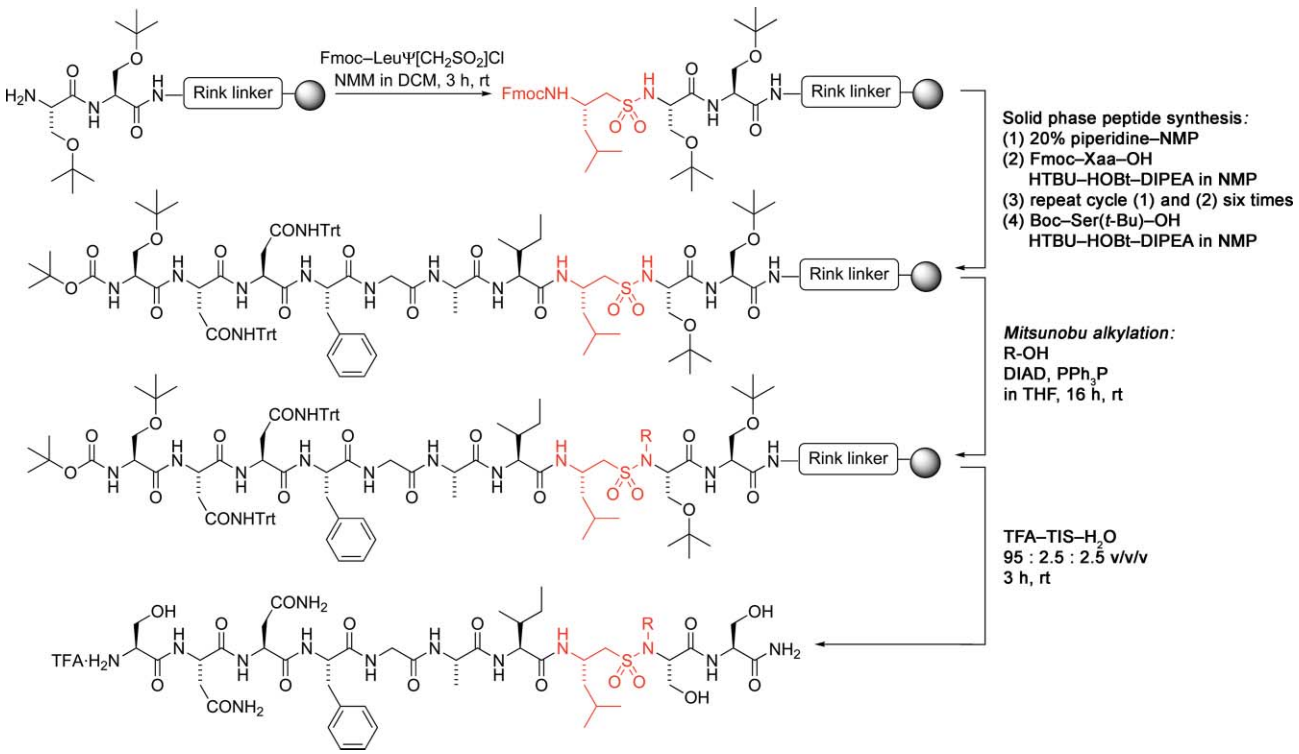

Scheme 1 Solid phase synthesis of the amylin(20–29) derivatives.

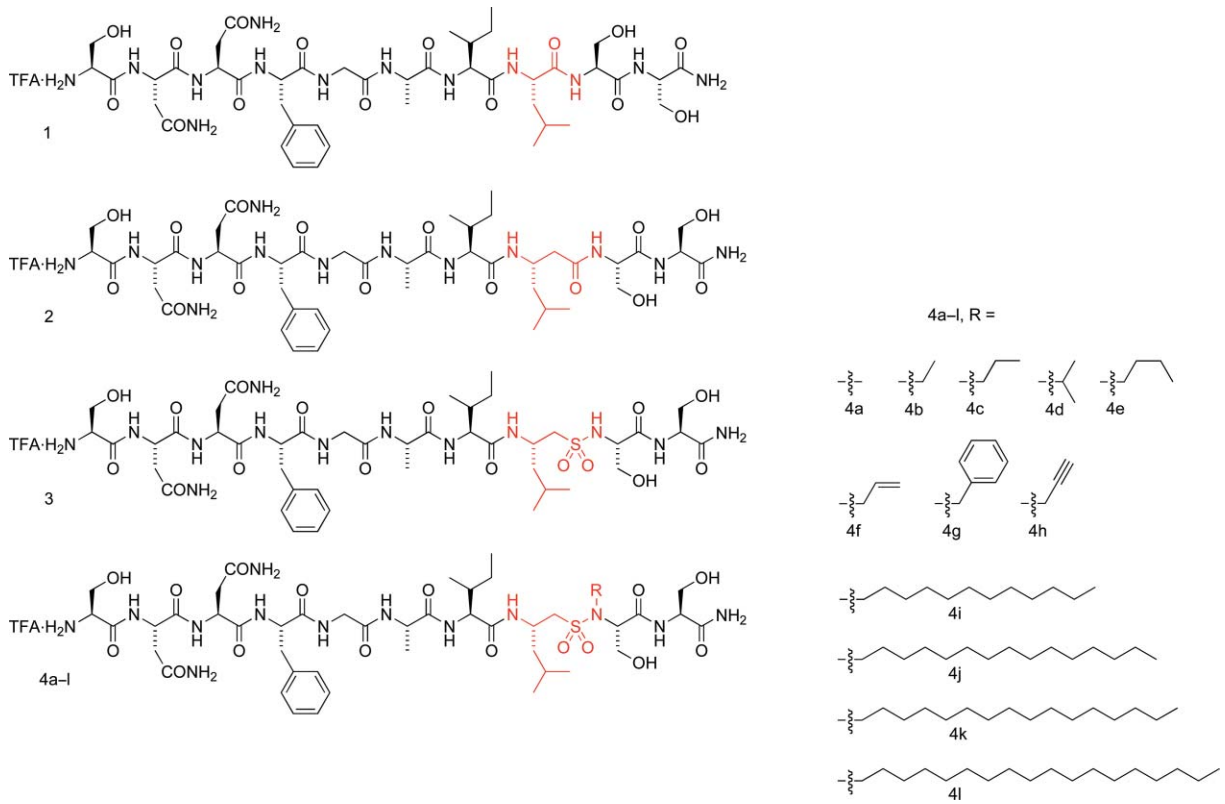

Fig. 2 Structures of the amylin(20–29) derivatives synthesized in this study.

yields (44–85%). The peptides were purified by HPLC and characterized by mass spectrometry (Table 1).

The rationale for incorporation of a β-leucine ((*S*)-3-amino-5-methylhexanoic acid) residue at position 27 of amylin(20–29) (compound **2**) was based on earlier observations by Moriarty and Raleigh.[22] They found that fibril formation of amylin(20–29) was particularly sensitive to modifications of the amide of serine 28. Thus, it was expected that residues at position 27 would affect the chemical and physical properties of this amine moiety, which resulted in the design and synthesis of the β-peptidosulfonamide–peptide hybrid **3** and the corresponding *N*-alkylated derivatives **4a**–**l**.

Gel formation

Native amylin(20–29) **1** was used as a reference peptide. This peptide was dissolved in 0.1% TFA–H_2O (10 mg mL^{-1}) and rapidly formed an opaque gel. The presence of amyloid fibrils was verified by transmission electron microscopy (TEM) (Fig. 3A and 4A) and β-sheet formation was confirmed by the amide I absorption at *circa* 1630 cm^{-1} in the Fourier transform infrared spectrum (FTIR)[23] (Table 2) and by circular dichroism (CD) (Table 2), either in a TFA buffer (Fig. 5A) or in a phosphate buffer (Fig. 6A). All these observations were in agreement with literature data[24] and our earlier experiments.[8]

Table 1 EI-MS, MALDI-TOF and HPLC data of the amylin derivatives

	EI-MS $[M + H]^+$	MALDI-TOF $[M + Na]^+$		
Peptide	Found (calcd)	Found (calcd)	R_t (TFA buffer)/min	R_t (TEAP buffer)/min
1	1008.80 (1008.50)	1030.501 (1030.482)	17.63 (C8)	2.67 (C8)
2	1022.70 (1022.53)	1044.546 (1044.511)	17.22 (C8)	1.58 (C8)
3	1058.17 (1058.49)	1080.645 (1080.472)	17.60 (C8)	2.41 (C8)
4a	1072.70 (1072.51)	1095.470 (1094.492)	18.12 (C8)	3.77 (C8)
4b	1086.60 (1086.53)	1108.471 (1108.511)	18.72 (C8)	6.02 (C8)
4c	1100.70 (1100.54)	1122.586 (1122.522)	18.93 (C8)	6.71 (C8)
4d	1100.70 (1100.54)	1122.522 (1122.522)	19.50 (C8)	8.33 (C8)
4e	1114.90 (1114.56)	1136.528 (1136.542)	20.53 (C8)	10.50 (C8)
4f	1098.80 (1098.53)	1120.519 (1120.512)	19.22 (C8)	7.43 (C8)
4g	1148.60 (1148.54)	1170.470 (1170.522)	21.13 (C8)	11.58 (C8)
4h	1096.60 (1096.51)	1118.518 (1118.492)	18.98 (C8)	6.65 (C8)
4i	1226.85 (1226.68)	1248.563 (1248.662)	24.40 (C4)	17.60 (C4)
4j	1268.70 (1268.73)	1290.549 (1290.712)	24.38 (C4)	20.27 (C4)
4k	1282.85 (1282.75)	1304.591 (1304.732)	26.82 (C4)	21.25 (C4)
4l	1310.75 (1310.78)	1332.538 (1332.762)	26.88 (C4)	22.77 (C4)

Table 2 Physicochemical properties of the amylin derivatives

Peptide	Gel formation	Morphology	FTIR/cm^{-1} [a]	CD [b]
1	Yes (<10 min), opalescent	Amyloid fibrils	1631 (s)	β-Sheet
2	Yes (<10 min), turbid	Lamellar sheets	1677 (s), 1639 (s)	Min. λ 217 nm, max. λ 195 nm
3	Yes (~40 min), turbid	Helical ribbons progressing to closed tubes	1679 (s), 1639 (s)	Random coil
4a	Yes (~5 h), translucent	No aggregates visible	1678 (s), 1645 (s)	Random coil
4b	Yes (>24 h), translucent	No aggregates visible	1670 (s), 1644 (m)	N.d.
4c	Yes (~1 h), translucent	Twisted double fibers	1676 (s), 1644 (w)	N.d.
4d	Clear solution	Long thin fibers	1676 (s), 1644 (w)	N.d.
4e	Yes (>24 h), translucent	Long broad fibers	1674 (s), 1645 (s)	Random coil
4f	Yes (~30 min), turbid	Broad branched fibers	1670 (s), 1645 (s)	N.d.
4g	Yes (~30 min), turbid	Twisted lamellar sheets	1677 (s), 1631 (w)	Random coil
4h	Yes (~30 min), translucent	Twisted long fibers	1670 (s), 1644 (w)	N.d.
4i	Yes (~45 min), translucent	Entangled fibers	1674 (s), 1643 (s)	Collagen-like triple helix
4j	Yes (~1 h), translucent	Entangled fibers	1667 (s), 1644 (s)	N.d.
4k	Yes (~20 min), translucent	Entangled fibers	1667 (s), 1644 (s)	Random coil
4l	Clear solution	Entangled fibers	1678 (s), 1643 (s)	N.d.

[a] Typical amide I absorption frequency (cm^{-1}) 1630: aggregated β-sheets; 1640: unordered structure; 1675: antiparallel β-sheet, according to ref. 23*b*. [b] CD spectra are shown in Fig. 5 and 6.

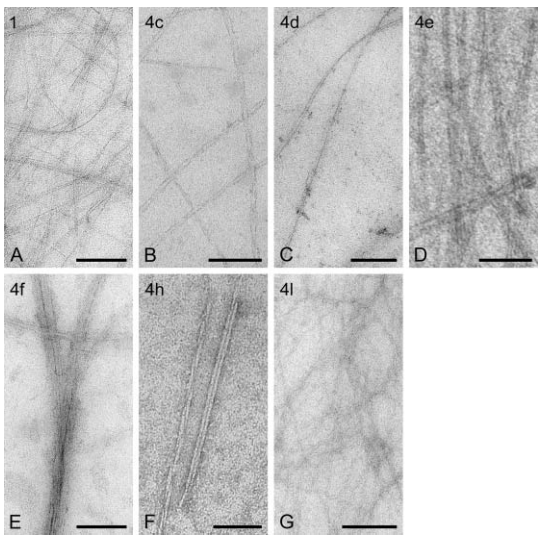

Fig. 3 TEM pictures of the amylin(20–29) derivatives. (A) **1**; (B) **4c**; (C) **4d**; (D) **4e**; (E) **4f**; (F) **4h** and (G) **4l**. Scale bar represents 100 nm.

Amylin(20–29) Leu27→βLeu **2** did not rapidly dissolve in 0.1% TFA–H_2O (10 mg mL^{-1}) and formed instantaneously a highly viscous turbid solution/suspension which gelled upon standing (Table 2). Amyloid fibrils were not observed by TEM, instead, long slightly twisted lamellar sheets were visible (Fig. 4B). The absence of amyloid fibrils was corroborated by FTIR (Table 2), since the characteristic peak at 1630 cm^{-1} of the amide I absorption was absent. Also, CD spectroscopy (Fig. 5A and 6A) confirmed the absence of amyloid fibrils as the predominant supramolecular structure since it showed a complete different behavior (a minimum at λ 217 nm, a maximum at λ 195 nm) of **2** compared to native amylin(20–29). Interestingly, introduction of a single methylene moiety in the peptide backbone was able to disrupt the hydrogen bonding network leading to the folding into (anti)parallel β-sheets and ultimately amyloid fibrils. Apparently, the hydrophobicity and the intrinsic self-assembly of this peptide was responsible for the formation of the observed supramolecular assemblies, as recently described for depsipeptide derivatives of amylin(20–29).[8b]

Amylin(20–29) Leu27→LeuΨ[CH_2SO_2] **3** was dissolved in 0.1% TFA–H_2O and the turbid solution was gelled after 40 min. This β-peptidosulfonamide–peptide hybrid aggregated into helical ribbons and some of these ribbons progressed into closed peptide nanotubes of up to 12 μm in length, as judged by TEM (Fig. 4C). Based on the FTIR and CD data (Table 2) it was concluded that **3** was present as a random coil. The absence of any secondary structure resulted from the ability of the sulfonamide moiety to act as a structure-breaker as was observed earlier in helical hexameric- and nonameric β-peptides.[14] However, the intrinsic chirality of the peptide backbone and the presence of hydrogen bond donors and the π–π stacking of the aromatic phenylalanine side chains[25] resulted in the formation of supramolecular helical ribbons.

The *N*-alkylated sulfonamides **4a** (methyl) and **4b** (ethyl) rapidly dissolved in 0.1% TFA–H_2O and the clear solution formed a translucent gel after standing for 5 and 24 h, respectively. However, neither the presence of amyloid fibrils nor supramolecular aggregates was observed by electron microscopy. This was rather unexpected since gelation or an increased viscosity was always accompanied with the presence of aggregates (amyloid fibrils, supramolecular assemblies).[8] These peptides were the first two examples in which the essential amide of serine 28 was not able to form an hydrogen bond (*vide supra*). On the other hand, both alkyl groups had a small contribution to the overall hydrophobicity of the peptide, which did not result in a pronounced amphiphilic character. Thus, the absence of the essential hydrogen bond abrogated any form of aggregation. This was confirmed by FTIR (Table 2) and CD (Fig. 5B and 6B), which showed the typical spectra of a random coil conformation with respect to **4a** and **4b**.

The *N*-alkylated sulfonamides **4c** (propyl) and **4d** (isopropyl) were dissolved in 0.1% TFA–H_2O and the clear solution of **4c** formed a translucent gel within 1 h. However, a solution of **4d** did not form a gel and remained clear. As visualized by TEM, both peptides formed fibers (Fig. 3B and C) with a different morphology. Fibers formed by **4c** were twisted in contrast to those formed by **4d** which were long, thin and non-twisted. An identical gelation behavior was found for the *N*-alkylated sulfonamide **4e** (butyl); after 24 h a translucent gel was obtained. As judged by electron microscopy, long and broad fibers were

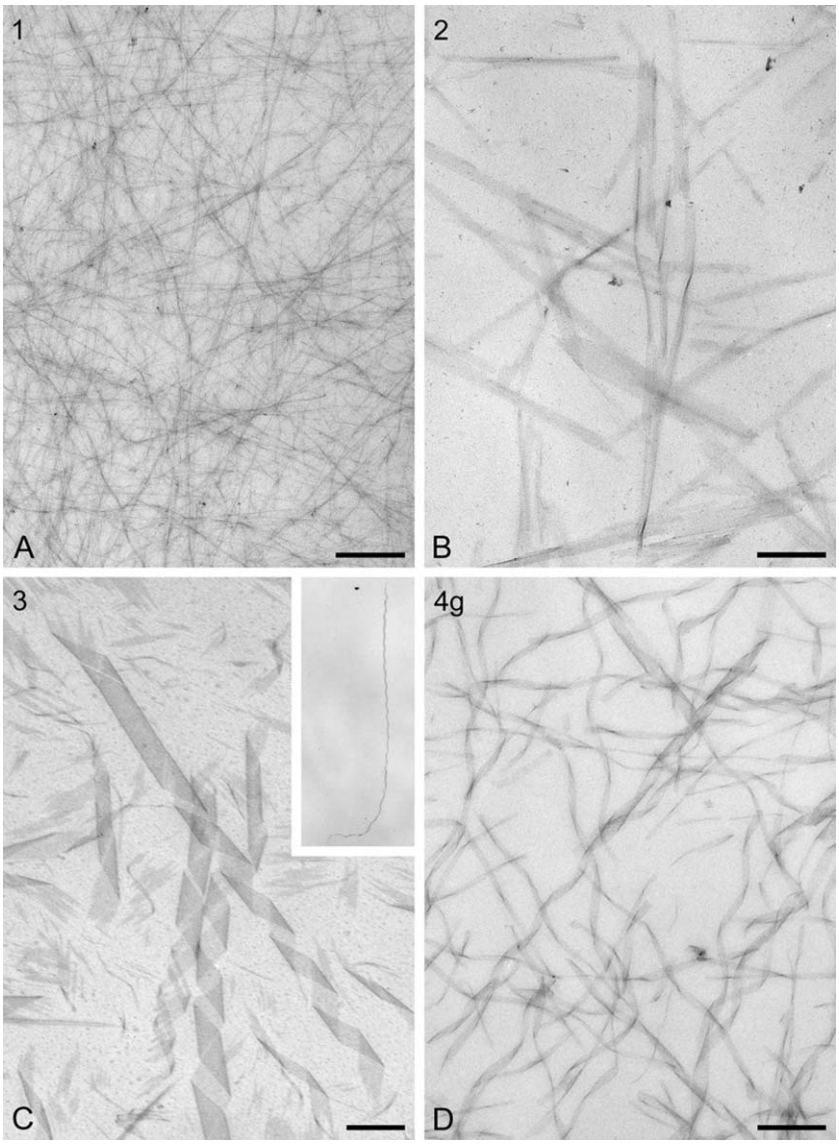

Fig. 4 TEM pictures of the amylin(20–29) derivatives. (A) **1**; (B) **2**; (C) **3** and (D) **4g**. Scale bar represents 500 nm.

observed (Fig. 3D). These longer alkyl chains increased the overall hydrophobicity substantially which apparently was responsible for the observed fiber formation. Both FTIR and CD spectra confirmed that this aggregation process was not based on amyloid fibril formation (absence of the characteristic peak at 1630 cm^{-1} of the amide I absorption), since these measurements strongly support a random conformation (Table 2 and Fig. 5B and 6B).

The *N*-alkylated sulfonamides **4f** (allyl), **4g** (benzyl) and **4h** (propargyl) were synthesized to study the presence of either an alkenyl/alkynyl chain or an aryl moiety on their gelation behavior. These amylin derivatives gelled the solution rapidly (within 30 min) and only in the case of **4h** was a clear gel formed. Sulfonamide **4f** aggregated into broad branched (or intertwined) fibers (Fig. 3E) although it did not adopt a secondary structure as shown by FTIR (Table 2). Also sulfonamide **4h** was unstructured in solution as judged by FTIR (Table 2), but here long twisted fibers were visible (Fig. 3F). This was in sharp contrast to the *N*-benzyl sulfonamide **4g**, which showed twisted lamellar sheets and in some cases they were visible as closed tubes (Fig. 4D). However, **4g** did not adopt any secondary structure in solution as was clear from FTIR- (Table 2) and CD-measurements (Fig. 5B and 6B). From the literature is it known that aromatic moieties *e.g.* benzyl groups (side chain of phenylalanine: π–π stacking) are important determinants of supramolecular folding either into amyloid fibrils or peptide nanotubes.[25,26]

The *N*-alkylated sulfonamides **4i** (C12, dodecyl), **4j** (C15, pentadecyl), **4k** (C16, hexadecyl) and **4l** (C18, octadecyl) were insoluble in 0.1% TFA–H_2O. Therefore, 1.0 mg of each derivative was dissolved in 10 μL DMSO (clear solution) and diluted with 90 μL 0.1% TFA–H_2O. The obtained clear aqueous solutions formed a translucent gel within 1 h, except sulfonamide **4l** which remained as a clear solution (even after 24 h). Generally, these fatty alcohol peptide amphiphiles formed fibers as shown (only for the C18 derivative, **4l**) in Fig. 3G. Due to the presence of the saturated lipid moieties, the driving force of self-assembly of these alkylated sulfonamides was changed from

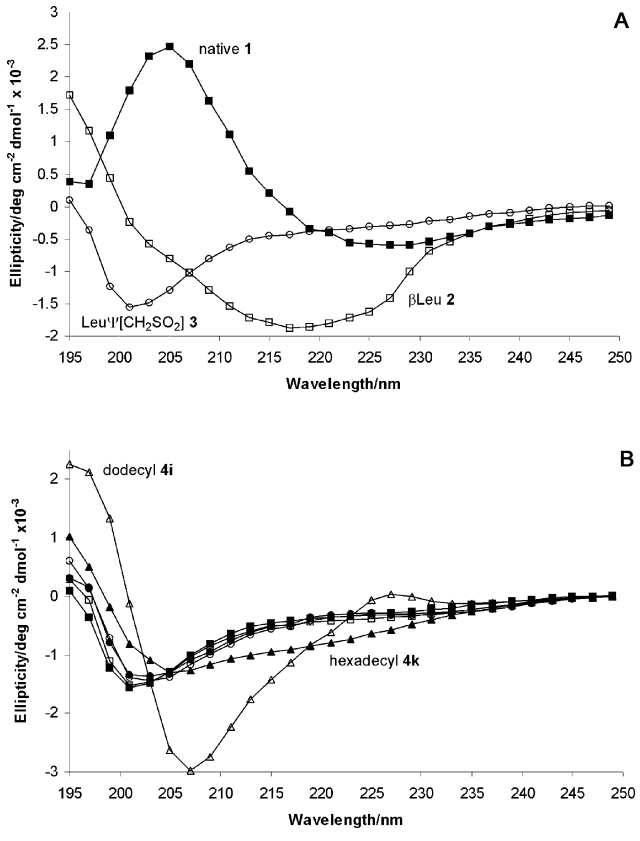

Fig. 5 CD spectra of the amylin(20–29) derivatives in 0.1% TFA–H_2O. (A) Upper frame ■: **1**; □: **2**; ○: **3**. (B) Lower frame ■: **3**; □: **4a**; ○: **4e**; ●: **4g**; △: **4i** and ▲: **4k**.

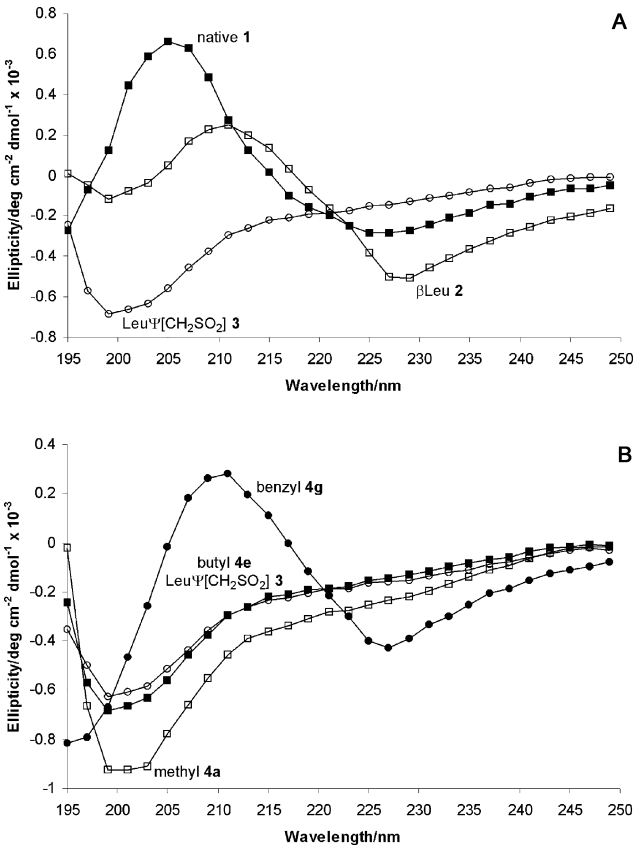

Fig. 6 CD spectra of the amylin(20–29) derivatives in phosphate buffer at pH 7.4. (A) Upper frame ■: **1**; □: **2**; ○: **3**. (B) Lower frame: ■: **3**; □: **4a**; ○: **4e**; ●: **4g**.

peptide-driven (hydrogen bonding, hydrophobic side-chain–side-chain interactions) to lipid-driven. Typical amide absorption peaks, characteristic for strong hydrogen bonding-based peptide–peptide interactions, were absent in the FTIR spectra. Representative examples of lipid-driven self-assembly have been published by Fields and coworkers[27a] and others.[27b] Fields *et al.* described the design and synthesis of small peptide collagen mimics by N-terminal derivatization of proline-rich peptide sequences with saturated fatty acid acyl chains.[28] Furthermore, evidence for the lipid-driven self-assembly of compound **4i** was found in its typical CD spectrum (Fig. 5B), showing a maximum at λ 227 nm and a minimum at λ 207 nm. However, increasing the length of the acyl chain (**4k**) strongly determined the overall folding and nullified apparently any contribution of specific peptide–peptide interaction.

Discussion

Amyloid fibrils are characterized by the (anti)parallel organization of β-pleated sheets,[29,30] which lead to a reduced solubility of the protein and to the formation of deposits of amyloid plaques. On one hand amyloid formation in living organisms is a highly undesirable process and is a (co)causitive factor in several diseases *e.g.* Alzheimer's disease (AD), Parkinson's disease (PD), transmissible spongiform encephalopathies (scrapie, BSE and Creutzfeldt–Jakob disease) and late onset diabetes (diabetes type II).[31] On the other hand, amyloid formation can also be exploited in the design of self-assembled bionanomaterials. In our studies we used as a model peptide the 20–29 sequence of amylin (H–Ser–Asn–Asn–Phe–Gly–Ala–Ile–Leu–Ser–Ser–NH_2), which is known as an amyloidogenic sequence from native amylin,[32] which itself is involved in type II diabetes.[33] Here, we describe our efforts in the design of material-like properties of peptide nanotubes and hydrogelators, based on the intrinsic self-assembly of an amyloid-derived peptide.

A characteristic hydrogen bonding network of an antiparallel β-sheet is shown in Fig. 7A. As shown by FTIR (Table 2), TEM (Fig. 3A and 4A) and CD (Fig. 5A and 6A), amylin(20–29) **1** formed amyloid fibrils as expected. Based on this H-bonding network, several models of how helical tapes, ribbons and fibrils/fibers are formed have been postulated in the literature.[34,35] Also, rationally designed peptide nanotubes[36,37] helical pores,[38] peptidomimetics of cross β-sheet assemblies[39a,b] and *de novo* designed β-sheet-forming strands,[39c] short tau peptides,[40] amyloid fibril mimics[41] or amino acid-/peptide-derived organo-[42] and hydrogelators[17,43] are based on this model of antiparallel β-sheet.

The substitution of Leu27 by (*S*)-3-amino-5-methylhexanoic acid (β-leucine) in amylin(20–29) resulted in β-peptide–α-peptide hybrid **2**, which did not fold into characteristic amyloid fibrils (*vide supra*). The absence of amyloid fibrils may be explained by the out of register hydrogen bonding pattern as induced by the incorporation of an extra methylene moiety (Fig. 7B). However, this peptide was found to be a hydrogelator and the lamellar sheets observed by TEM were somewhat surprising. Apparently, the

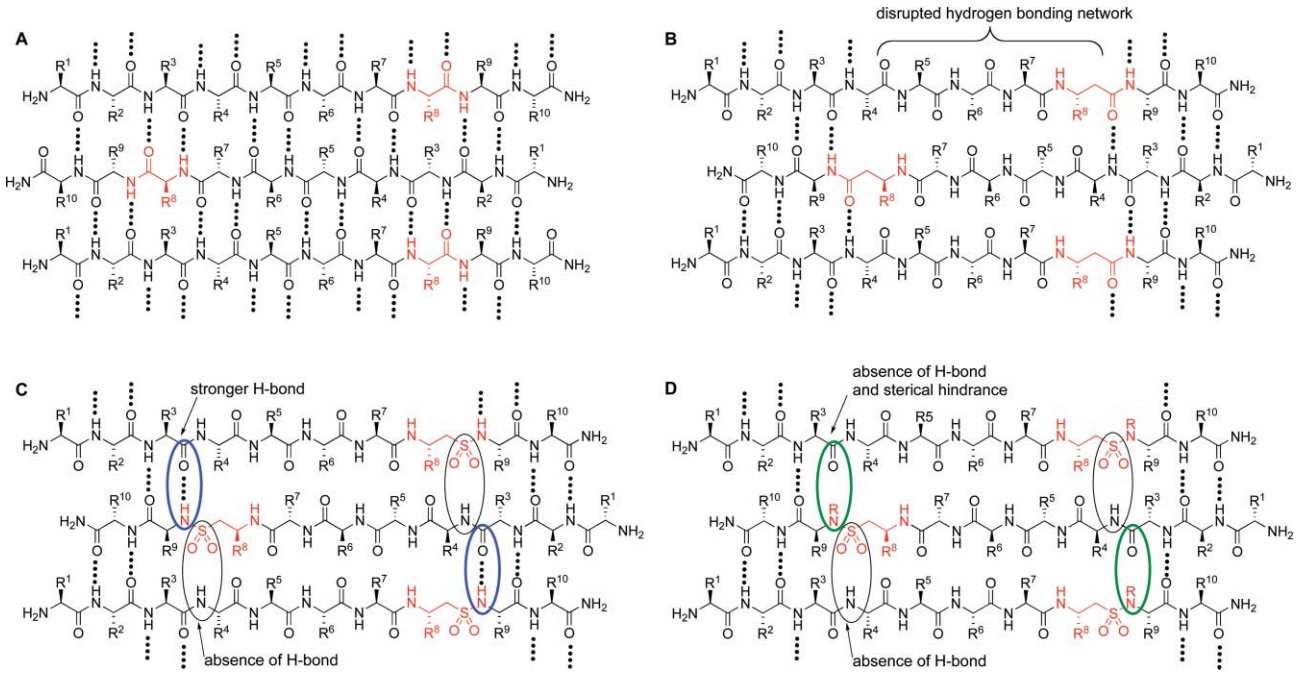

Fig. 7 Structural representation of a β-pleated sheet: (A) native amylin(20–29) **1**; (B) incorporation of a β-peptide: **2**; (C) replacement of an amide bond by an sulfonamide moiety: **3**; (D) alkylation of the sulfonamide N*H*: **4a**–**l**.

driving force to form these sheets is merely based on hydrophobic side chain interactions[8] rather than hydrogen bonds, which is in line with the FTIR (Table 2) and CD (Fig. 5A and 6B) data.

Substitution of a peptide amide bond by a sulfonamide, to obtain β-peptidosulfonamide–peptide hybrid **3**, introduces a stronger hydrogen bond donor but a weaker hydrogen bond acceptor. As viewed by TEM (Fig. 4C), this amylin(20–29) derivative was found to form helical ribbons and closed peptide nanotubes. As is the case with β-peptide–α-peptide hybrid **2**, β-peptidosulfonamide–peptide hybrid **3** cannot form an ideal hydrogen bonding network as depicted in Fig. 7C. Although, the FTIR spectra of **2** and **3** are almost identical, which may imply that the sulfonamide moiety plays a minor role in the formation of the observed peptide nanotubes, due to its dichotomy as hydrogen bond donor and/or acceptor (*vide supra*)[14] it is surprising to observe the lamellar twist of this derivative as opposed to **2**. Recently, a similar supramolecular morphology has been reported by us in the case of amylin(20–29) peptides, in which all important hydrogen bonds involved in amyloid formation have been removed.[8b] Formation of the peptide nanotubes has been explained as an interplay of an increase of the overall hydrophobicity of the peptide construct and side-chain–side-chain interactions.

Alkylation of the sulfonamide N*H* (**4a**–**l**) induces sterical hindrance and removes a strong hydrogen bond donor, these simultaneous alterations of the amide bond properties make the antiparallel alignment into a β-sheet motif highly unfavorable (Fig. 7D). The concept of *N*-methylation has successfully been applied in the design of soluble β-sheet mimics that inhibit amyloid formation.[44] The absence of fibrils (TEM) in case of the N–Me and N–Et sulfonamides **4a** and **4b**, respectively, was in agreement with data from the literature. However, incorporation of longer alkyl chains, generally increases the hydrophobicity and ultimately leads to the formation of a peptide amphiphile. The aggregation behavior of the peptide amphiphiles (**4c**–**4l**) is determined by the hydrophobicity and length of the alkyl chain (lipid-driven) since the morphology of the aggregates is generally the same (Fig. 3B–G). There is, however, one exception: *N*-benzyl sulfonamide **4g**, which self-assembles into twisted lamellar sheets and (closed) peptide tubes (Fig. 4D). Represented as an antiparallel β-sheet, the side chain of phenylalanine can be oriented co-planarly to the sulfonamide *N*-benzyl for optimal π–π stacking interactions (Fig. 8A). Recently, these π–π stacking interactions have been defined as important determinants in supramolecular folding either into amyloid fibrils or peptide nanotubes.[25,37] Moreover, a piece of indirect evidence for these π–π stacking interactions (as oriented in an antiparallel β-sheet) in the case *N*-benzyl sulfonamide **4g**, is the presence of a signal at 1631 cm^{-1} in the FTIR spectrum, since in all other *N*-alkylated sulfonamides this signal is absent.

In conclusion, we describe here the successful synthesis of backbone-modified amylin(20–29) derivatives in which one amide bond is replaced by a sulfonamide functionality. The sulfonamide moiety is regiospecifically alkylated with a diverse set of alcohols featuring the Mitsunobu reaction on the solid support. These amylin derivatives did not form amyloid fibrils, however, they self-assembled into diverse supramolecular assemblies such as lamellar sheets, helical ribbons, peptide nanotubes and close networks of entangled fibers. The compounds describes here will find application as hydrogelators and newly designed bionanomaterials (insulated wires, drug delivery devices, nanoreactors) based on small peptides and peptidomimetics.

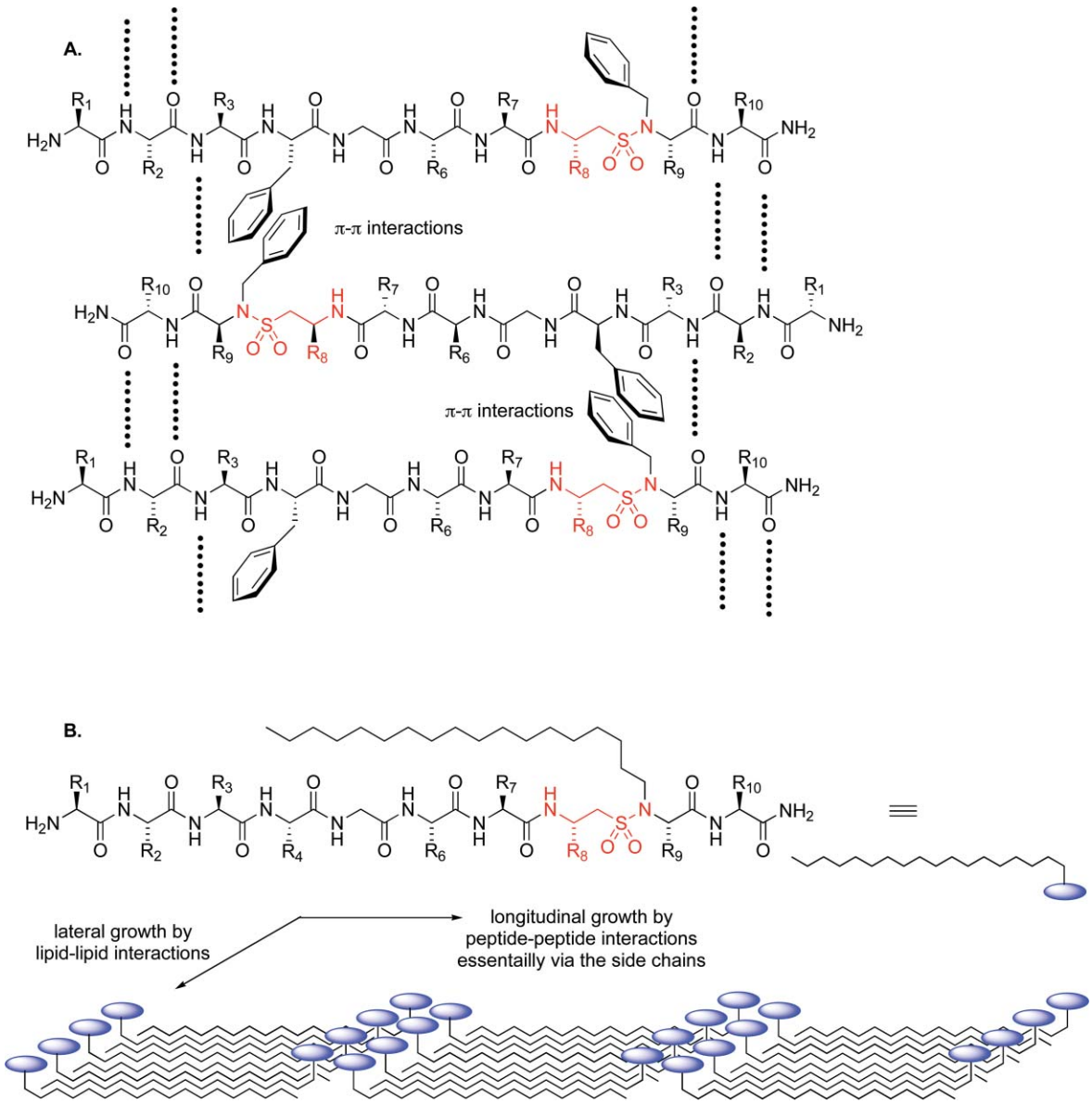

Fig. 8 (A) Structural representation of a β-pleated sheet in the case of sulfonamide **4g**; strong influence of π–π interactions as determinants of the supramolecular folding morphology. (B) Pictorial respresentation of the lipid-driven self-assembly of the peptide amphiphiles.

Material and methods

General

Chemicals were obtained from commercial sources and used without further purification, unless stated otherwise. Peptide grade solvents used for solid phase peptide synthesis were purchased form Biosolve and were stored on 4 Å MS. Peptides were synthesized on a Applied Biosystems 433A peptide synthesizer. Analytical HPLC runs were performed on a Shimadzu automated HPLC system equipped with a UV/VIS detector operating at 220/254 nm and an evaporative light scattering detector (Polymer Laboratories ELS 1000). Peptides were purified using a Gilson HPLC workstation. Infrared spectra were recorded on a BioRad FTS6000 spectrometer. CD-spectroscopy was performed on a Olis RSM-1000 spectrometer.

Peptide synthesis

Peptides **1** and **2** were synthesized using the FastMoc protocol on a 0.25 mmol scale[20] on Argogel® Fmoc-Rink-Amide resin to obtain the C-terminally amidated peptides.[45] Each synthetic cycle consisted of *N*-α-Fmoc removal by a 10 min treatment with 20% piperidine in NMP, a 6 min NMP wash, a 45 min coupling step with 1.0 mmol of preactivated Fmoc amino acid in the presence of 2 equivalents DIPEA, and a 6 min NMP wash. *N*-α-Fmoc Amino acids were activated *in situ* with 1.0 mmol HBTU–HOBt (0.36 M in NMP)[46] in the presence of DIPEA (2.0 mmol). The peptides were detached from the resin and deprotected by treatment with TFA–H_2O–TIS 95 : 2.5 : 2.5 v/v/v for 3 h. The peptides were precipitated with MTBE–hexane 1 : 1 v/v at −20 °C and finally lyophilized from *tert*-butanol–H_2O 1 : 1 v/v.

Synthesis of β-peptidosulfonamide–peptide hybrid 3

Fmoc–Ser(*t*-Bu)–Ser(*t*-Bu)–NH-Rink-Amide resin (0.25 mmol) was washed with CH_2Cl_2 (3 × 2 min, 10 mL) and NMP (3 × 2 min, 10 mL) then treated with 20% piperidine–NMP (3 × 8 min, 10 mL) to remove the Fmoc group. After washing the resin with NMP (3 × 2 min, 10 mL), the solvent system was changed into CH_2Cl_2 by extensive washing with CH_2Cl_2 (6 × 2 min, 10 mL).[14] Then, Fmoc–LeuΨ[CH_2SO_2]Cl[19] (422 mg, 1.0 mmol, 4 equiv.) was coupled to the α-amino group with NMM (165 μL, 1.5 mmol. 6 equiv.) as base in CH_2Cl_2 (10 mL). The coupling was followed by the Kaiser test[47] and the bromophenol blue test (BPB)[48] and was found to be complete after 3 h. The resin was washed with CH_2Cl_2 (3 × 2 min, 10 mL) and NMP (6 × 2 min, 10 mL). Peptide synthesis was continued following the Fmoc–*t*-Bu solid phase peptide synthesis protocols. The final amino acid was coupled as its *N*-α-Boc protected derivative (Boc–Ser(*t*-Bu)–OH). Subsequently, a small portion of the resin was treated with TFA–TIS–H_2O 95 : 2.5 : 2.5 v/v/v to remove all protecting groups and to detach the peptide form the resin. The β-peptidosulfonamide–peptide hybrid **3** was precipitated with MTBE–hexane 1 : 1 v/v at −20 °C and finally lyophilized from *tert*-butanol–H_2O 1 : 1 v/v.

N-Alkylation of the sulfonamide on the solid phase

Alkylation of the sulfonamide moiety, to obtain the *N*-alkylated β-peptidosulfonamide–peptide hybrids **4a**–**l**, was performed on the solid phase in the presence of DIAD (4 equiv.), triphenylphosphine (4 equiv.) and the alcohol (8 equiv.) in freshly distilled THF. As a typical example, for the synthesis of **4i**, resin-bound fully protected peptide **3** (200 mg, 0.06 mmol) was washed with CH_2Cl_2 (3 × 10 mL, 2 min) followed by THF (3 × 10 mL, 2 min). Then, the resin was treated with triphenylphosphine (63 mg, 0.24 mmol), 1-dodecanol (90 mg, 0.48 mmol) and DIAD (47 μL, 0.24 mmol) in THF (10 mL) for 16 h. Finally, the resin was extensively washed with THF (3 × 10 mL, 2 min) and CH_2Cl_2 (3 × 10 mL, 2 min). The *N*-alkylated β-peptidosulfonamide–peptide hybrids were deprotected and cleaved from the resin with TFA–TIS–H_2O 95 : 2.5 : 2.5 v/v/v for 3 h. The crude β-peptidosulfonamide–peptide hybrids were precipitated in cold MTBE–hexane 1 : 1 v/v at −20 °C and lyophilized from *tert*-BuOH–H_2O 1 : 1 v/v.

Peptide purification

Preparative HPLC runs were performed on a Gilson HPLC workstation equipped with an UV/VIS detector operating at 220/254 nm. Columns used for preparative peptide purification were either a LiChroCART 250–20 CN (10 μm particle size, 100 Å pore size, *l*: 250 mm, i.d.: 10 mm) semipreparative column running at a flow rate of 5 mL min^{-1} or an Adsorbosphere XL C8 (10 μm particle size, 90 Å pore size, *l*: 250 mm, i.d. 22 mm) column running at a flow rate of 10 mL min^{-1}. The buffer used was 0.1% TFA in H_2O (buffer A) and 0.1% TFA in CH_3CN–H_2O 95 : 5 v/v (buffer B) using a linear gradient from 100% buffer A to 100% buffer B in 60 min.

Peptide characterization

Analytical HPLC runs were performed on a Shimadzu automated HPLC system equipped with a UV/VIS detector operating at 220/254 nm and an evaporative light scattering detector (Polymer Laboratories ELS 1000). Columns used for purity analyses were either an Adsorbosphere XL C8 (5 μm particle size, 90 Å pore size, *l*: 250 mm, i.d.: 4.6 mm) column or an Adsorbosphere XL C4 (5 μm particle size, 300 Å pore size, *l*: 250 mm, i.d.: 4.6 mm) column using a linear gradient from 100% buffer A to 100% buffer B in 40 min at a flow rate of 1 mL min^{-1}. Two buffer systems were used, the first buffer system was: buffer A: 0.1% TFA in H_2O and buffer B: 0.085% TFA in CH_3CN–H_2O 95 : 5 v/v and the second buffer system was: buffer A: 50 mM triethylamine–H_3PO_4 in H_2O–CH_3CN (8 : 2 v/v) pH 2.25 and buffer B was 50 mM TEA–H_3PO_4 in CH_3CN–2-propanol–H_2O (10 : 9 : 1 v/v/v) pH 2.25. Peptides were characterized using electrospray mass spectrometry (EI-MS) and was performed on a Shimadzu LCMS-QP8000 single quadruple bench top mass spectrometer operating in a positive ionization mode and MALDI-TOF analyses on a Kratos Axima CFR apparatus, with human angiotensin II as external reference (monoisotopic $(M + H)^+$: 1046.542) and α-cyano-4-hydroxycinnamic acid or 2,5-dihydroxybenzoic acid as matrices.

Gelation experiments

Each peptide sample (10 mg) was dissolved in 0.1% TFA–H_2O (1 mL) at 25 °C. The aggregation state was determined by eye at regular time intervals by tilting the test tube and check if the solution still flowed. If no flow was observed, gelation was said to have taken place.

Transmission electron microscopy

A peptide gel/solution (10 mg peptide per mL in 0.1% TFA–H_2O) aged for three weeks (10 μL) was placed on a carbon coated copper grid. After 15 min, any excess of peptide was removed by washing the copper grid on a drop of demi-water (this was repeated four times) Finally, the samples were stained by methylcellulose–uranyl acetate and dried on air. The samples were visualized under a Jeol 1200 EX transmission electron microscope operating at 60 kV. The magnification ranged from 10 000 to 60 000 times.

Fourier transform infrared spectroscopy

A peptide gel solution (10 mg peptide per mL in 0.1% TFA–H_2O) aged for three weeks (100 μL) was lyophilized and subsequently resuspended in D_2O (150 μL) and lyophilized. This treatment was repeated twice. The lyophilized peptides were dried over P_2O_5 in high vacuum for 24 h. A peptide sample was mixed with KBr and pressed into a pellet. The optical chamber was flushed with dry nitrogen for 5 min before data collection started. The interferograms from 1000 scans with a resolution of 2 cm^{-1} were averaged and corrected for H_2O and KBr. The experimental FTIR spectra were correlated with data from the literature.[23]

Circular dichroism spectroscopy

CD spectra were measured at 1.0 nm intervals in the range of 195–250 nm as the average of 20 runs using a spectral band width of 2.0 nm in 0.5 mm cuvettes thermostated at 20 °C with the optical chamber continually flushed with dry N_2 gas. The spectra were measured in 0.1% TFA in H_2O. The concentrations (1 mg mL^{-1})

were determined on the basis of the calculated molecular mass of the purified lyophilized peptides as the TFA salt. A peptide sample was dissolved in 0.1% TFA in H_2O and stored for 4 d at 4 °C prior to analysis. A second buffer system[49] was used in the CD experiments (1.8 mM NaH_2PO_4, 8.2 mM Na_2HPO_4 in 100 mM NaCl at pH 7.4) at the same concentration and conditions as described for the TFA buffer.

Acknowledgements

These investigations were supported by the council for Chemical Sciences of the Netherlands-Organization for Scientific Research (CW–NWO). We thank Annemarie Dechesne for measuring the MALDI-TOF spectra.

References

1 (*a*) S. Deechongkit, P. E. Dawson and J. W. Kelly, *J. Am. Chem. Soc.*, 2004, **126**, 16762; (*b*) D. J. Gordon and S. C. Meredith, *Biochemistry*, 2003, **42**, 475.
2 J. A. W. Kruijtzer, L. J. F. Hofmeyer, W. Heerma, C. Versluis and R. M. J. Liskamp, *Chem.–Eur. J.*, 1998, **4**, 1570.
3 (*a*) K. Burgess, D. S. Linthicum and H. Shin, *Angew. Chem., Int. Ed. Engl.*, 1995, **34**, 907; (*b*) J.-M. Kim, Y. Bi, S. J. Paikoff and P. G. Schultz, *Tetrahedron Lett.*, 1996, **37**, 5305; (*c*) K. Burgess, J. Ibarzo, D. S. Linthicum, D. H. Russell, H. Shin, A. Shitankoon, R. Totani and A. J. Zhang, *J. Am. Chem. Soc.*, 1997, **119**, 1556; (*d*) A. Boeijen and R. M. J. Liskamp, *Eur. J. Org. Chem.*, 1999, 2127; (*e*) A. Boeijen, J. van Ameijde and R. M. J. Liskamp, *J. Org. Chem.*, 2001, **66**, 8454.
4 J. A. W. Kruijtzer, D. J. Lefeber and R. M. J. Liskamp, *Tetrahedron Lett.*, 1997, **38**, 5335.
5 Y. Fu, J. Bieschke and J. W. Kelly, *J. Am. Chem. Soc.*, 2005, **127**, 15366.
6 (*a*) D. B. A. de Bont, G. D. H. Dijkstra, J. A. J. den Hartog and R. M. J. Liskamp, *Bioorg. Med. Chem. Lett.*, 1996, **6**, 3035; (*b*) D. B. A. de Bont, W. J. Moree and R. M. J. Liskamp, *Bioorg. Med. Chem.*, 1996, **4**, 667; (*c*) D. B. A. de Bont, K. M. Sliedregt-Bol, L. J. F. Hofmeyer and R. M. J. Liskamp, *Bioorg. Med. Chem.*, 1999, **7**, 1043.
7 J. van Ameijde and R. M. J. Liskamp, *Tetrahedron Lett.*, 2000, **41**, 1103.
8 (*a*) D. T. S. Rijkers, J. W. M. Höppener, G. Posthuma, C. J. M. Lips and R. M. J. Liskamp, *Chem.–Eur. J.*, 2002, **8**, 4285; (*b*) R. C. Elgersma, T. Meijneke, G. Posthuma, D. T. S. Rijkers and R. M. J. Liskamp, *Chem.–Eur. J.*, 2006, **12**, 3714.
9 D. Seebach, M. Overhand, F. N. M. Kuhnle, B. Martinoni, L. Oberer, U. Hommel and H. Widmer, *Helv. Chim. Acta*, 1996, **79**, 913.
10 R. P. Cheng, S. H. Gellman and W. F. DeGrado, *Chem. Rev.*, 2001, **101**, 3219.
11 S. H. Gellman, *Acc. Chem. Res.*, 1998, **31**, 173.
12 D. Seebach, A. K. Beck and D. J. Bierbaum, *Chem. Biodiversity*, 2004, **1**, 1111.
13 (*a*) M. C. F. Monnee, M. F. Marijne, A. J. Brouwer and R. M. J. Liskamp, *Tetrahedron Lett.*, 2000, **41**, 7991; (*b*) M. C. F. Monnee, M. F. Marijne, A. J. Brouwer and R. M. J. Liskamp, *Tetrahedron Lett.*, 2001, **42**, 965.
14 (*a*) R. de Jong, D. T. S. Rijkers and R. M. J. Liskamp, *Helv. Chim. Acta*, 2002, **85**, 4230; (*b*) R. de Jong, D. T. S. Rijkers and R. M. J. Liskamp, in *Innovation and Perspectives in Solid Phase Synthesis & Combinatorial Libraries*, ed. R. Epton, Mayflower Worldwide Ltd., Kingswinford, England, 2004, p. 151.
15 (*a*) D. W. P. M. Löwik, S. J. E. Mulders, Y. Cheng, Y. Shao and R. M. J. Liskamp, *Tetrahedron Lett.*, 1996, **37**, 8253; (*b*) D. W. P. M. Löwik, M. D. Weingarten, M. Broekema, A. J. Brouwer, W. C. Still and R. M. J. Liskamp, *Angew. Chem., Int. Ed.*, 1998, **37**, 1846; (*c*) A. J. Brouwer, H. J. van der Linden and R. M. J. Liskamp, *J. Org. Chem.*, 2000, **65**, 1750; (*d*) R. M. J. Liskamp and J. A. W. Kruijtzer, *Mol. Diversity*, 2004, **8**, 79.
16 (*a*) S. Zhang, D. M. Marini, W. Hwang and S. Santoso, *Curr. Opin. Chem. Biol.*, 2002, **6**, 865; (*b*) K. Rajagopal and J. P. Schneider, *Curr. Opin. Struct. Biol.*, 2004, **14**, 480.
17 (*a*) L. A. Estroff and A. D. Hamilton, *Chem. Rev.*, 2004, **104**, 1201; (*b*) M. de Loos, B. L. Feringa and J. H. van Esch, *Eur. J. Org. Chem.*, 2005, 3615; (*c*) N. M. Sangeetha and U. Maitra, *Chem. Soc. Rev.*, 2005, **34**, 821.
18 (*a*) S. C. Miller and T. S. Scanlan, *J. Am. Chem. Soc.*, 1997, **119**, 2301; (*b*) J. F. Reichwein and R. M. J. Liskamp, *Tetrahedron Lett.*, 1998, **39**, 1243; (*c*) J. F. Reichwein, B. Wels, J. A. W. Kruijtzer, C. Versluis and R. M. J. Liskamp, *Angew. Chem., Int. Ed.*, 1999, **38**, 3684.
19 A. J. Brouwer, M. C. F. Monnee and R. M. J. Liskamp, *Synthesis*, 2000, 1579.
20 C. G. Fields, D. H. Lloyd, R. L. Macdonald, K. M. Otteson and R. L. Noble, *Peptide Res.*, 1991, **4**, 95.
21 O. Mitsunobu, *Synthesis*, 1983, 1.
22 D. F. Moriarty and D. P. Raleigh, *Biochemistry*, 1999, **38**, 1811.
23 (*a*) S. Krimm and J. Bandekar, *Adv. Protein Chem.*, 1986, **38**, 181; (*b*) M. Jackson and H. H. Mantsch, *Crit. Rev. Biochem. Mol. Biol.*, 1995, **30**, 95.
24 (*a*) K. Tenedis, M. Waldner, J. Berhagen, W. Fischle, M. Bergmann, M. Weber, M.-L. Merkle, W. Voelter, H. Brunner and A. Kapurniotu, *J. Mol. Biol.*, 2000, **295**, 1055; (*b*) R. Azriel and E. Gazit, *J. Biol. Chem.*, 2001, **276**, 34156.
25 (*a*) S. M. Tracz, A. Abedini, M. Driscoll and D. P. Raleigh, *Biochemistry*, 2004, **43**, 15901; (*b*) Y. Porat, Y. Mazor, S. Efrat and E. Gazit, *Biochemistry*, 2004, **43**, 14454; (*c*) O. S. Maki, E. Atkins, P. Sikorski, J. Johansson and L. C. Serpell, *Proc. Natl. Acad. Sci. U. S. A.*, 2005, **102**, 315.
26 D. M. Chung, Y. Dou, P. Baldi and J. S. Nowick, *J. Am. Chem. Soc.*, 2005, **127**, 9998.
27 (*a*) P. Forns, J. L. Lauer-Fields, S. Gao and G. B. Fields, *Biopolymers*, 2000, **54**, 531; (*b*) D. W. P. M. Löwik, J. C. Linhardt, P. J. H. M. Adams and J. C. M. van Hest, *Org. Biomol. Chem.*, 2003, **1**, 1827.
28 Y.-C. Yu, M. Tirrell and G. B. Fields, *J. Am. Chem. Soc.*, 1998, **120**, 9979.
29 (*a*) A. T. Petkova, Y. Ishii, J. J. Balbach, O. N. Antzutkin, R. D. Leapman, F. Delaglio and R. Tycko, *Proc. Natl. Acad. Sci. U. S. A.*, 2002, **99**, 16742; (*b*) R. Tycko, *Biochemistry*, 2003, **42**, 3151.
30 (*a*) A. Kishimoto, K. Hasegawa, H. Suzuki, H. Taguchi, K. Namba and M. Yoshida, *Biochem. Biophys. Res. Commun.*, 2004, **315**, 739; (*b*) R. Krishnan and S. L. Lindquist, *Nature*, 2005, **435**, 765; (*c*) R. Nelson, M. R. Sawaya, M. Balbirnie, A. O. Madsen, C. Riekel, R. Grothe and D. Eisenberg, *Nature*, 2005, **435**, 773; (*d*) C. Ritter, M.-L. Maddelein, A. B. Siemer, T. Lührs, M. Ernst, B. H. Meier, S. J. Saupe and R. Riek, *Nature*, 2005, **435**, 844; (*e*) M. Tanaka, P. Chien, K. Yonekura and J. S. Weisman, *Cell*, 2005, **121**, 49; (*f*) C. M. Dobson, *Nature*, 2005, **435**, 747; (*g*) S. W. Liebman, *Nat. Struct. Mol. Biol.*, 2005, **12**, 567.
31 (*a*) G. G. Glenner and C. W. Wong, *Biochem. Biophys. Res. Commun.*, 1984, **122**, 1131; (*b*) C. Soto, *Nat. Rev. Neurosci.*, 2003, **4**, 49; (*c*) C. M. Dobson, *Science*, 2004, **304**, 1259.
32 P. Westermark, U. Engstrom, K. H. Johnson, G. T. Westermark and C. Betsholtz, *Proc. Natl. Acad. Sci. U. S. A.*, 1990, **87**, 5036.
33 J. W. M. Höppener, B. Ahrén and C. J. M. Lips, *New Engl. J. Med.*, 2000, **343**, 411.
34 (*a*) A. Aggeli, I. A. Nyrkova, M. Bell, R. Harding, L. M. Carrick, T. C. B. McLeish, A. N. Semenov and N. Boden, *Proc. Natl. Acad. Sci. U. S. A.*, 2001, **98**, 11857; (*b*) C. W. G. Fishwick, A. J. Beevers, L. M. Carrick, C. D. Whitehouse, A. Aggeli and N. Boden, *Nano Lett.*, 2003, **3**, 1475; (*c*) K. Pagel, T. Vagt and B. Koksch, *Org. Biomol. Chem.*, 2005, **3**, 3843; (*d*) K. Pagel, S. C. Wagner, K. Samedov, H. von Berlepsch, C. Böttcher and B. Koksch, *J. Am. Chem. Soc.*, 2006, **128**, 2196.
35 (*a*) D. M. Marini, W. Hwang, D. A. Lauffenburger, S. Zhang and R. D. Kamm, *Nano Lett.*, 2002, **2**, 295; (*b*) W. Hwang, D. M. Marini, R. D. Kamm and S. Zhang, *J. Chem. Phys.*, 2003, **118**, 389.
36 (*a*) S. Matsumura, S. Uemura and H. Mihara, *Chem.–Eur. J.*, 2004, **10**, 2789; (*b*) X. Gao and H. Matsui, *Adv. Mater.*, 2005, **17**, 2037.
37 (*a*) M. Reches and E. Gazit, *Science*, 2003, **300**, 625; (*b*) K. Lu, J. Jacob, P. Thiyagarajan, V. P. Conticello and D. G. Lynn, *J. Am. Chem. Soc.*, 2003, **125**, 6391; (*c*) M. Yemini, M. Reches, J. Rishpon and E. Gazit, *Nano Lett.*, 2005, **5**, 183; (*d*) N. Kol, L. Adler-Abramovich, D. Berlam, R. Z. Shneck, E. Gazit and I. Rousso, *Nano Lett.*, 2005, **5**, 1343; (*e*) J. Dong, J. E. Shokes, R. A. Scott and D. G. Lynn, *J. Am. Chem. Soc.*, 2006, **128**, 3540.
38 V. Percec, A. E. Dulcey, V. S. K. Balagurusamy, Y. Miura, J. Smidrkal, M. Peterca, S. Nummelin, U. Edlund, S. D. Hudson, P. A. Heiney, H. Duan, S. N. Magonov and S. A. Vinogradov, *Nature*, 2004, **430**, 764.
39 (*a*) H. A. Lashuel, S. R. LaBrenz, L. Woo, L. C. Serpell and J. W. Kelly, *J. Am. Chem. Soc.*, 2000, **122**, 5262; (*b*) S. Deechongkit, E. T. Powers, S.-L. You and J. W. Kelly, *J. Am. Chem. Soc.*, 2005, **127**, 8562; (*c*) M. S.

Lamm, K. Rajagopal, J. P. Schneider and D. J. Pochan, *J. Am. Chem. Soc.*, 2005, **127**, 16692.
40 W. J. Goux, L. Kopplin, A. D. Nguyen, K. Leak, M. Rutkofsky, V. D. Shanmuganandam, D. Sharma, H. Inouye and D. A. Kirschner, *J. Biol. Chem.*, 2004, **279**, 26868.
41 C. Madhavaiah and S. Verma, *Chem. Commun.*, 2004, 638.
42 (*a*) C. Zhan, P. Gao and M. Liu, *Chem. Commun.*, 2005, 462; (*b*) J. H. Jung, J. A. Rim, S. J. Lee and S. S. Lee, *Chem. Commun.*, 2005, 468.
43 (*a*) C. Boettcher, B. Schade and J.-H. Fuhrtop, *Langmuir*, 2001, **17**, 873; (*b*) M. Suzuki, S. Owa, M. Kimura, A. Kurose, H. Shirai and K. Hanabusa, *Tetrahedron Lett.*, 2005, **46**, 303.
44 (*a*) L. O. Tjenberg, J. Näslund, F. Lindqvist, J. Johansson, A. R. Karlström, J. Thyberg, L. Terenius and C. Norstedt, *J. Biol. Chem.*, 1996, **271**, 8545; (*b*) C. Soto, E. M. Sigurdsson, L. Morelli, R. A. Kumar, E. M. Castono and B. Frangione, *Nat. Med.*, 1998, **4**, 822; (*c*) E. Hughes, R. M. Burke and A. J. Doig, *J. Biol. Chem.*, 2000, **275**, 25109; (*d*) D. J. Gordon, K. L. Sciarretta and S. C. Meredith, *Biochemistry*, 2001, **40**, 8237.
45 H. Rink, *Tetrahedron Lett.*, 1987, **28**, 3787.
46 R. Knorr, A. Trzeciak, W. Bannwarth and D. Gillesen, *Tetrahedron Lett.*, 1989, **30**, 1927.
47 E. Kaiser, R. L. Colescott, C. D. Bossinger and P. I. Cook, *Anal. Biochem.*, 1970, 34595.
48 V. Krchňák, J. Vágner, P. Šafář and M. Lebl, *Collect. Czech. Chem. Commun.*, 1988, **53**, 2542.
49 T. T. Ashburn and P. T. Lansbury, Jr., *J. Am. Chem. Soc.*, 1993, **115**, 11012.